Scientia cum Industria

Special Issue
7° CONGRESSO INTERNACIONAL DE TECNOLOGIAS PARA O MEIO AMBIENTE

PLATINUM OPEN ACCESS
eISSN 2318-5279

Original Research

Assessment of the addition of mineral fillers on the flammability, morphological and thermal properties of polypropylene

Keiti Gilioli Tosin[1]*
Andrezza Piroli Tonello[2]
Matheus Poletto[3]

[1,3] Postgraduate Program in Engineering of Processes and Technologies (PGEPROTEC) - University of Caxias do Sul, RS, Brazil.
[2] University of Caxias do Sul, RS, Brazil.
* Corresponding author: kgtosin@ucs.br

Received: November 17, 2023
Revised: June 10, 2024
Accepted: November 22, 2024
Published: January 30, 2025

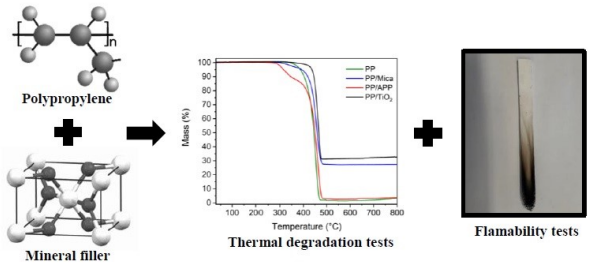

Abstract: Fire safety is a growing concern in the materials industry, leading to a study exploring the sustainable use of mineral fillers in polymeric materials. Polypropylene (PP) plates were developed with non-halogenated flame retardants, such as muscovite mica, titanium dioxide, and ammonium polyphosphate (APP). Sample preparation involved a Haake rheometer and compression molding. Material characterization included scanning electron microscopy, thermogravimetry, flammability testing, thermal conductivity, and specific gravity. Morphological analysis showed filler's dispersion in the PP matrix. Thermogravimetric analysis revealed higher thermal degradation temperatures in samples with inorganic fillers compared to PP. The pyrolysis index of PP/TiO_2 and PP/Mica was roughly one-fourth that of PP/APP and about half that of the PP sample. During fire reaction testing, none of the samples exhibited flame retardant behavior according to UL-94, but PP/TiO_2 plates formed a char on the surface. The additives do not alter the thermal conductivity of the plates, making them suitable as thermal insulators. Specific gravity evaluation revealed a 3.3% increase in density for PP/APP plates compared to PP, while PP/Mica and PP/TiO_2 plates increased 28.4% and 24.8%, respectively. These findings suggest the potential of the plates as insulating materials in the construction industry, highlighting TiO_2's additive due to its char-forming properties.

Keywords: Flammability, mineral fillers, muscovite mica, polypropylene, titanium dioxide.

Introduction

The increased use of polymeric materials as a substitute for metal components in industries that require high standards of fire protection has led to a greater demand for high-performance flame retardants [1]. Flame retardants are materials with self-extinguishing properties. They are categorized into different groups, such as halogenated, phosphorus-based, nitrogen-based, boron-based, silicone-based, biochar, and metal oxide, depending on their chemical composition [2].

Despite having a high potential as flame retardants, halogenated compounds are considered bioaccumulative and can cause numerous diseases in humans and animals [3]. One of these harmful effects is carcinogenicity and the tendency to generate organic pollutants [2]. These detrimental additives also pose complications in the recycling process, as they are used in sectors such as electricity, electronics, automotive, and construction [4]. Furthermore, the incorporation of brominated flame retardants can adversely affect the mechanical properties of polypropylene, including its tensile strength, flexural strength, and impact resistance [5].

Current regulations already prohibit the use of various halogenated flame retardants. In Europe, there is a transition towards the use of phosphorus-based flame retardants, which are less toxic. The most widely employed phosphorus-based flame retardant is ammonium polyphosphate (APP), an inorganic compound formed from polyphosphoric acid and ammonia [6]. This additive is a type of intumescent flame retardant, which interrupts the polymer's combustion in its early stages, forming a char layer on the part. This layer protects the underlying material layers from the heat and flames, acting as a physical barrier that reduces the transfer of heat and mass between the gas phase and the condensed phase [7].

With the increasing fire safety requirements in end-use industries, the production of flame retardants has expanded into a multibillion-dollar industry [8]. The main types of flame retardants are inorganic, halogenated organic, and organophosphorus. Global consumption of flame retardants in plastics are about 48% correspond to inorganic flame

retardants, followed by 31% of halogenated flame retardants, 15% of organophosphorus flame retardants, and 6% of other types of flame retardants [9]. Thus, compounds based on mineral fillers make up a significant portion of flame-retardant additives. This is due to their cost, which is considerably lower compared to organic solutions, making it economically viable to combine them with common materials [10].

Furthermore, an advantage of using mineral fillers is that the gasses produced during combustion do not exhibit corrosion or acidity, making them suitable for indoor use [11]. The endothermic decomposition of these additives has the effect of cooling the solid or condensed phase and results in the release of water or carbon dioxide [12]. Moreover, the inorganic residue that remains after the filler decomposition can serve as a thermal barrier, insulating against external sources of heat. Some mineral fillers serve a dual function, enhancing both flame-retardant characteristics and antibacterial properties [13].

Titanium dioxide (TiO_2) is a material used in energy storage devices due to its characteristics such as affordable cost, surface-to-volume ratio, electrical and thermal stability, electroactive surface structure, dielectric constant, non-toxicity, and the ability to assume multivalent oxidation states [14]. Moreover, it can exhibit flame-retardant properties, which vary depending on the applied concentration, particle size, and surface area [15].

Mica is a raw material used in the production of high-temperature insulators for nuclear and military industries, as well as in aircraft construction, instrument manufacturing, and mechanical engineering. From mica, products like paper, plastics, tapes, electric heating elements, and other items for the electrical industry are manufactured [16]. Muscovite, a variety of mica, and titanium dioxide are additives with the potential to be incorporated into polymers due to their inorganic nature and affordable cost [17,18].

The influence of adding fillers to polymers varies depending on the type of polymer matrix and the type of filler. Increasing the aspect ratio and stiffness of the matrix is reported to be beneficial for the elasticity modulus [19]. The composite becomes stiffer as the number of particulate fillers increases, an effect that is exploited in various mechanical components but can be disadvantageous in flexible coating applications due to reduced flexibility. Furthermore, a significant increase in the viscosity of the molten material is observed as the filler content increases [10].

Chen et al. [20] developed a compound of N-alkoxyamine containing zirconium phosphate (ZrP) nanosheets decorated with macromolecular intumescent flame retardant (MIFR), referred as RQMIFR-ZrP, combined with ammonium polyphosphate (APP) to impart flame retardant properties to polypropylene (PP). The addition of 6.3% by weight of RQMIFR-ZrP and 18.7% by weight of APP resulted in a UL-94 V-0 classification for PP, with a Limiting Oxygen Index (LOI) value of 39.5%. Additionally, measurements of the maximum heat release rate, total heat release, maximum CO production, and CO2 production decreased compared to the pure polymer.

Jo et al. [21] developed intumescent flame-retardant coatings for cotton/polyethylene terephthalate (C/PET) using a blend of ammonium polyphosphate (APP), pentaerythritol (PER), titanium dioxide (TiO_2), and an acrylic emulsion as a binder. Vertical flame tests were conducted on the samples, demonstrating an increased flame retardancy as TiO_2 content in the coatings increased (from 2.5 wt% to 10 wt%), with post-flame times recorded as nil. Furthermore, TiO_2 facilitated the formation of a compact char layer with no voids.

Furthermore, Almeida et al. [22] synthesized a mixture of recycled high-density polyethylene (rHDPE) and muscovite mica in various ratios. Hardness evaluation revealed that mica acted as a reinforcing component in the composite matrix when a 15 wt% content was used. Thermogravimetric analysis (TG) indicated that the composite with an 85 wt% rHDPE and 15 wt% mica ratio performed the best among the samples. Additionally, the decomposition rate peaks (DTG) showed slight variation, with deceleration observed as the mica ratio in the composite increased.

Considering the benefits of using mineral fillers, this study aims to utilize titanium dioxide and muscovite mica as low-toxicity flame retardant additives in PP, as well as to explore the potential of ammonium polyphosphate.

Experimental Section

The homopolymer polypropylene used in this work was supplied by Braskem (grade H 103) with a melt flow index of 40 g/10 min (230 °C/2.16 kg). Ammonium polyphosphate (APP), a non-halogenated commercial flame retardant, was produced by Clariant Indústria Química under the trade name Exolit AP 442, with a density of 1900 kg/m3, phosphorus content of 31wt% to 32wt%, and nitrogen content of 14 wt% to 15 wt%. Titanium dioxide (TiO_2) grade Ti-Pure® R-902 was obtained from DuPont, with a purity of 91%, an average particle size of 0.42 µm, and a density of 4.23 g/cm³. The muscovite mica (MICA LAMIL 3250) from Lamil has a density of 2.8 ± 2 g/cm³. The materials were mixed according to Table 1.

Table 1. Coding and formulation of the synthesized samples.

Sample	PP (wt.%)*	APP (wt.%)*	Mica (wt.%)*	TiO_2 (wt.%)*
PP	100	-	-	-
PP/APP	70	30	-	-
PP/Mica	70	-	30	-
PP/TiO_2	70	-	-	30

* % m/m.

To produce the samples, the materials were dried in an oven at 80°C for 4 hours. The filler incorporation content was maintained at 30 wt%, whereas flame retardant additives are typically used at loadings ranging from 5 to 30 wt% [23]. A

Haake rheometer was used for 5 min to facilitate the blending of PP and the evaluated fillers. The equipment operated at a speed of 60 rpm and a processing temperature of 180°C. After the components were mixed, plates with a thickness of 3.2 mm were molded using a press heated to 180°C and with a pressure of 5 tons for approximately 5 minutes.

The analysis was performed using a Field Emission Scanning Electron Microscope (FE-SEM) Mira Tescan 3 with an acceleration voltage of 15 kV. Cryogenic fracturing and gold coating were applied to the specimens. The thermogravimetric analysis was performed using a Shimadzu TGA-50 instrument, with a heating rate of 10 ºC/min and a temperature range of 23 - 800ºC, under a nitrogen atmosphere with a flow rate of 50 mL/min. Approximately 10 mg of the sample was used.

The TGA results were used to determine the mass loss rate and degradation stages. TGA results were subsequently employed to evaluate the degradation steps of the samples. Various parameters were utilized, including the ignition temperature (Ti), the burnout temperature (TB), the pyrolysis index (P), the ignition index (Di), the time corresponding to the maximum degradation rate (Tm), the time of ignition (Tig), the maximum rate of degradation and the mean rate of degradation. The ignition temperature was defined as the temperature at which the thermal degradation rate increases by 1% per minute, indicating the onset of the primary thermal degradation process. The burning temperature was defined as the temperature at which the thermal degradation rate decreases by 1% per minute, indicating the end of the thermal degradation process, as stipulated by Protásio et al. [24].

The pyrolysis index (P) was calculated using Equation 1, as referenced by Moon et al. [25] and Protásio et al. [24]. The ignition index (Di) was determined using Equation 2, established by Xiang-Guo et al. [26].

$$P = \frac{(\frac{dm}{dt})(\frac{dm}{dt})me}{T_i^2 \, X \, T_B} \quad (1)$$

$$D_i = \frac{(\frac{dm}{dt})max}{T_m \, X \, T_{ig}} \quad (2)$$

Where “(dm/dt) max” is the maximum rate of degradation (% min−1), “(dm/dt) me” the mean rate of degradation, “Ti” the ignition temperature (°C), “TB” the burnout temperature (°C), “Tm” the time corresponding to the maximum degradation rate (min) and “Tig” the time of ignition (min).

The material's flammability behavior was evaluated based on the UL-94 standard. Three specimens were prepared, with approximate dimensions of 3.2 mm in thickness, 13 mm in width, and 125 mm in length. The samples were positioned vertically using a clamp and a universal holder and then subjected to controlled flame exposure for two 10 second intervals. The burning of the specimen was assessed to determine if it extended to the clamp where the specimen was attached, and if there was any dripping or sparks that ignited the cotton placed at the base of the universal holder.

The thermal conductivity was determined following the ISO 8302 standard. This standard requires a system with a heating plate, a cooling plate, two temperature sensors, and a test specimen. The test specimen was placed between the two plates and then enclosed in an insulated casing. The device was activated at a temperature of 60°C and, once stabilized, temperature readings were recorded every 1 minute during the first 10 minutes, and then every 5 minutes until thermal stability of the cold plate was achieved over an additional five readings. The analysis was conducted in duplicate. To determine the thermal conductivity of the plates, calibrated equipment was used, meaning that the heat flux of the system (q) was obtained according to Equation 3.

$$q = \frac{k.\Delta T}{L} \quad (3)$$

Being “q” the heat flux of the system (W/m²), “k” the thermal conductivity of the sample (W/m·K), “ΔT” the temperature difference (T1-T2) and “L” the thickness of the sample (m).

Besides, the experimental thermal conductivity was compared to the theoretical models of Bruggerman, represented in Equation 4, and De Loor, described by Equation 5 [27].

$$K_c = \frac{K_m}{1-\emptyset_f} \quad (4)$$

$$K_c = \frac{K_m(1+\emptyset_f)}{1-2\emptyset_f} \quad (5)$$

Where “Kc” is the thermal conductivity of the material (W/m·K), “Km” the thermal conductivity of the matrix (PP) (W/m·K) and “□□” the volume fraction of the material.

To determine the specific gravity of the PP and the produced plates, test specimens with approximate dimensions of 2 cm x 2 cm, obtained from the previously compression-molded plate, were used. The specific gravity determination was conducted following ASTM D792-13. The samples were weighed on an analytical balance and subsequently immersed in ethanol and weighed again. The specific gravity was obtained as the average of three measurements for each of the sampled plates. The calculation to obtain the specific gravity value of the material was performed according to Equation 6.

$$\rho = \frac{(a.b)}{(a-c)} \quad (6)$$

Results and Discussion

Scanning electron microscopy

The morphology of the samples with the addition of fillers is shown in Figure 1. In general, the fillers were uniformly dispersed in the PP. The spherical-shaped APP showed weak interaction with the polymer matrix, as can be observed in Figure 1 (a). The lamellar-structured mica was well dispersed in the PP, and a certain degree of interaction between the two materials can be seen, as highlighted in the inset of Figure 1 (b). The morphology of the PP/TiO_2 plates is shown in Figure 1 (c). The oxide particles are small and have a spherical shape.

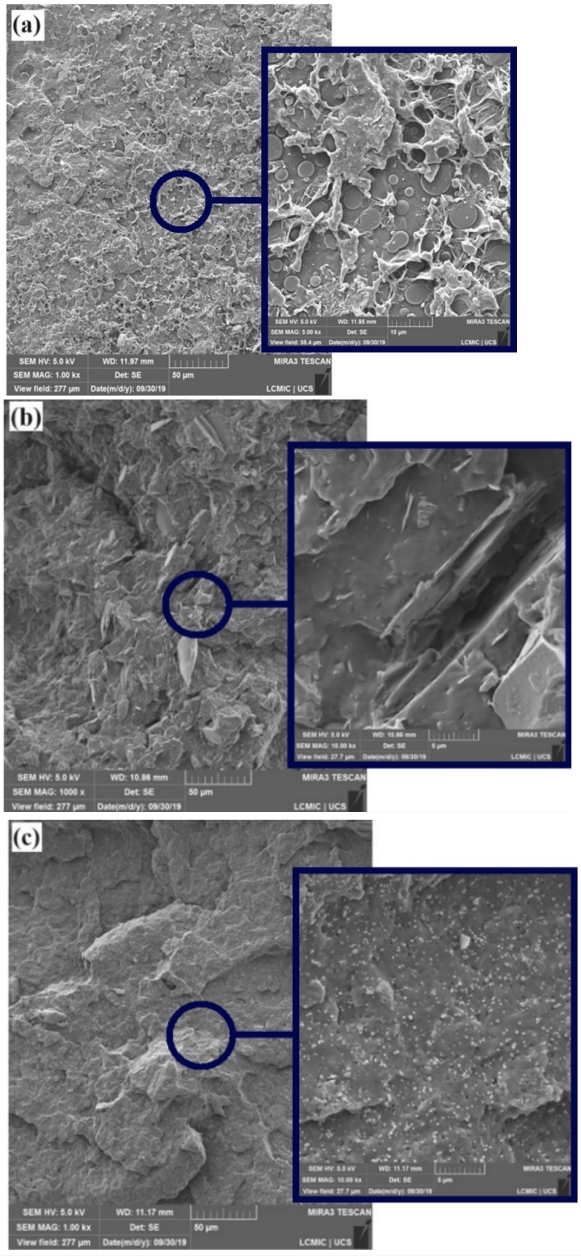

Figure 1. Micrographs (1000x) for PP/APP (a), PP/Mica (b), and PP/TiO_2 (c), with the detail (5000x) showing the interaction between PP/fillers.

The spherical shape of APP particles may not create an effective physical barrier against flame propagation. In contrast, the lamellar structure of mica can form a more efficient physical barrier, slowing both the spread of fire and the release of flammable gases. The good interaction between mica and PP also suggests that the resulting composite material may be more cohesive and heat resistant.

While the spherical morphology of the small TiO_2 particles allows for good dispersion, they may not be as effective in terms of flame retardancy as the lamellar structure of mica. However, TiO_2 particles can contribute to flame retardancy through other mechanisms, such as forming a protective oxide layer on the surface of the material when exposed to heat [28].

Thermogravimetric analysis

The thermogravimetric curves obtained for each of the plates with the addition of flame retardants are presented in Figure 2. An increase in the temperature at which PP initiates its degradation can be observed in the curves where TiO_2 were added. The oxide particles are small and have a spherical shape.

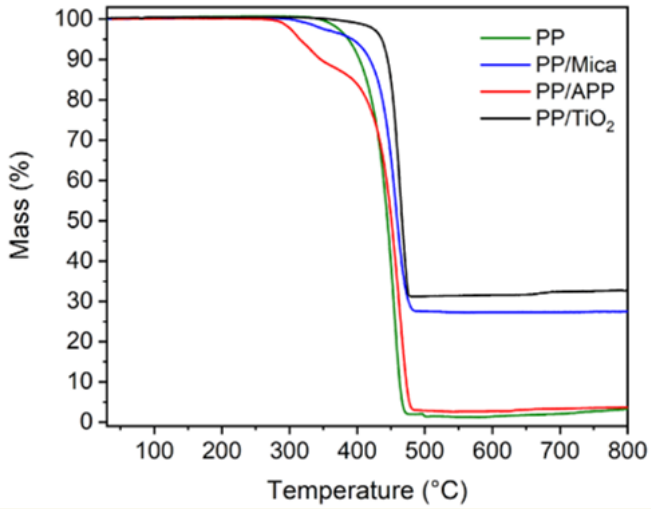

Figure 2. Thermogravimetric curves of the synthesized samples.

In Table 2, the data obtained through thermogravimetric curve analysis are presented. The PP exhibits a temperature of 3% mass loss at 376 °C and displays only one mass loss event, which occurs at a temperature of 454 °C. This mass loss event can be attributed to the cleavage of PP bonds [29]. In the PP/APP samples, two mass loss events were observed. The first event resulted in mass loss between 311 °C and 333 °C, and the second mass loss event occurred at 462 °C. Khanal et al. [18] explain that the first mass loss event in this material corresponds to the release of ammonia and water molecules, along with the formation of cross-linked phosphoric acid. The second event involves the dehydration of phosphoric acid and the loss of P4H10. The temperature at which this material lost 3% of its mass was 305 °C.

Table 2. Data obtained from thermal analyses.

Sample	$T_{3*\ \%}$ (°C)	$T_{peak\ 1}$ (°C)	$T_{peak\ 2}$ (°C)	Ash content ** (%)
PP	376	-	454	3.3
PP/APP	305	311/333	462	3.7
PP/Mica	363	340	454	27.4
PP/TiO_2	428	-	464	32.8

* The temperature at which a 3% mass loss occurs. **At 800 °C.

For the PP/Mica composite samples, the 3% mass loss occurred at a temperature of 363 °C. The first mass loss event in this material took place at 340 °C, and the second event occurred at 454°C. The remaining ash content for this material is 27.4% of the mass. According to Yang et al. [30], where the behavior of HDPE and mica composites was evaluated, the onset of thermal decomposition occurred at 304.1 °C. When analyzing the same parameter, Oliveira et al. [31] found an onset degradation temperature of 446.2 °C. In this instance, it was emphasized that when no compatibilizer was used in the blend, a higher amount of char was observed due to reduced interaction between the components, allowing the emission of degradation gasses.

In the PP/TiO_2 samples, the 3% mass loss occurred at a temperature of 428 °C. This material exhibited only one mass loss event, which occurred at a temperature of 464 °C. The remaining ash content for this material was 32.8%. Awang et al. [32] assessed the thermal behavior of composites based on polypropylene as a polymer matrix reinforced with rice husk inclinations when TiO_2 was added. The maximum degradation temperatures (Tmax) were 489.80 °C. This occurrence indicates that the composites with the addition of TiO_2 exhibit higher Tmax values and stability when compared to pure PP and the other composites. Additionally, the residual weight of most composites at 500°C increased when TiO_2 was incorporated, increasing the residual weight until 16.30%. These changes can be attributed to char formation. Besides, Ali et al. [33] analyzed the effect of incorporating TiO_2 into Poli (PVA/PLA) nanofilms. It was observed that the thermal stability of the nanocomposites increased with the addition of TiO_2, which can be attributed to an improvement in interfacial adhesion and compatibility between the TiO_2 polymer matrix and PVA/PLA.

From these data, it was possible to observe that the addition of TiO_2 allowed the degradation of PP to commence at a higher temperature compared to the other samples, given that TiO_2 is an oxide with high thermal stability [34,35]. The ash contents found in the PP/Mica and PP/TiO_2 samples can be attributed to the added inorganic fillers, considering that Mica and TiO_2 are inorganic materials. Since the amount of flame retardants added to each of the plates was 30 wt%, the values obtained show an apparent homogeneity. The lower ash content found in the PP/APP is because this compound degrades at temperatures close to 310 °C, as discussed earlier.

Table 3 presents some calculated parameters based on the TGA analysis. From the values presented, it is possible to observe that the highest Ti (ignition temperature) was for PP/TiO_2, and the lowest was for PP/APP. A low Ti value suggests that the material can burn more easily [36]. When examining the TB (burnout temperature), it is evident that the materials remained within a temperature range of around 480 °C, except for PP/APP, which resulted in 352 °C.

Higher combustion index values represent better fuel performance when burned [37]. In the case of this study, it would be the pyrolysis index since the TGA was conducted in an N_2 atmosphere. This is noticeable when comparing the PP/APP samples, a material that burned more easily, and PP/TiO_2, a material that proved to be more resistant among the samples. The PP/TiO_2 and PP/Mica exhibited a pyrolysis index approximately four times lower than PP/APP and about two times lower than the pure PP sample. Furthermore, the ignition index of PP/Mica and PP/TiO_2 remained lower when compared to pure PP and PP/APP, indicating that samples with mineral fillers have the potential as flame retardants.

Fire Reaction

The fire reaction test showed that none of the developed materials were able to achieve UL-94 classification, meaning that none of the developed materials can be considered flame-retardant. For all evaluated formulations, the test specimens ignited completely. The total burning time of PP was 107 ± 9s. The addition of the different flame retardants studied reduced the total burning time when compared to PP, except for PP/

Table 3. Values of ignition temperature (Ti), burnout temperature (TB), time of ignition (Tig), time corresponding to the maximum degradation rate (Tm), the maximum rate of degradation and the mean rate of degradation (dm/dt), the pyrolysis index (P), the ignition index (Di).

Sample	T_i (°C)	T_B (°C)	T_{ig}(min)	T_m (min)	(dm/dt) max (%/min)	(dm/dt) mean (%/min)	$Px10^{-7}$ ($\%^2min^{-2}°C^{-3}$)	$Dix10^{-2}$ ($\%min^{-3}$)
PP	363.7	474.1	34.9	44.1	23.8	1.2	4.6	1.5
PP/APP	291.2	352	26.3	43.6	19.5	1.2	7.8	1.7
PP/Mica	391.5	484.1	36.2	42.8	17.1	0.9	2.1	1.1
PP/TiO_2	422	479.2	40.9	45.2	24.9	0.8	2.3	1.3

APP, which remained very close (105 ± 5 s). The UL-94 test outcomes align with the burnout temperature of the samples, demonstrating that all materials maintained a temperature range of approximately 480°C. As mentioned, an exception was observed with PP/APP, which exhibited a lower burnout temperature of 352 °C.

In the PP/APP sample, the material exhibited fluidity upon contact with fire, and a significant amount of material dripping occurred, like the melting of a candle. Despite APP being commercially used in some formulations as a flame retardant, this additive, when combined with PP, did not prove effective in delaying or suppressing the combustion of the sample. This fact can also be visualized in Table 3, where the PP/APP achieved the worst results between the samples. The PP/Mica and PP/TiO_2 samples had similar total burning times (63 ± 4 and 64 ± 1 s, respectively). However, both samples ignited approximately 40 seconds faster than the PP or PP/APP sample.

Despite that, it was possible to observe a layer of soot formed on the specimen when in contact with fire for the PP/TiO_2 sample, as seen in Figure 3. This soot may indicate the beginning of char layer formation, which contributes to protecting the material from the effects of fire, as it prevents oxygen from further fueling the combustion process.

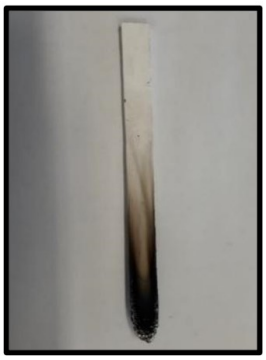

Figure 3. Formation of char in the PP/TiO_2 sample.

Thermal Conductivity

To calculate the thermal conductivity value of the samples in this study, the heat flux for the polypropylene was first obtained, using a thermal conductivity value of 0.20 W/mK [38]. By using Equation 3, a heat flux value "q" of 1190 W/m2 was determined for the system. This value served as the basis for calculating the thermal conductivity of the plates where flame retardants were added. The tests were conducted in duplicate. Table 4 shows that there was an increase in the thermal conductivity of the samples when compared to the thermal conductivity value for PP found in the literature. The increase was 12%, 24.5%, and 25.5% for PP/APP, PP/Mica, and PP/TiO_2, respectively. These results indicate that these materials can be used as thermal insulators since the thermal conductivity was not significantly affected by the incorporation of additives.

Table 4. Thermal conductivity values obtained for each material.

	Material	Thermal Conductivity (W/mK)
	PP/APP	
L*	0.0027 m	0.224 ± 0.007
ΔT**	14.27 K	
q***	1190 Wm^{-2}	
	PP/Mica	
L*	0.0027 m	0.249 ± 0.004
ΔT**	12.82 K	
q***	1190 Wm^{-2}	
	PP/TiO_2	
L*	0.0027 m	0.251 ± 0.001
ΔT**	12.55 K	
q***	1190 Wm^{-2}	

Thickness. ** Temperature variation. *** Heat flux of the system.

For comparative purposes, materials used in buildings, such as gypsum plasterboard and common bricks, have thermal conductivities of approximately 0.17 W/mK and 0.72 W/mK, respectively [38]. The values obtained for the thermal conductivity of the PP plates with flame retardants are quite close to materials like white gypsum plaster and sand (0.22 W/mK) and white gypsum plaster and vermiculite (0.25 W/mK), which are widely used in the construction industry [39]. Furthermore, the Brazilian standard ABNT NBR 15220 specifies thermal conductivities between 0.35 and 0.12 W/mK for plasterboard and pressed wood-derived boards, respectively, considering specific masses of 0.750 and 0.500 g/cm³, in that order.

Leng et al. [40] established the thermal conductivity of pure epoxy resin thermosets being 0.28 W/mK. To enhance the thermal properties, various formulations of ammonium polyphosphate (APP) and graphitic carbon nitride (g-C3N4) were introduced into the epoxy (EP) thermosets. The thermal conductivity of EP/CN-APP reached 0.56 W/mK. Zhang et al. [41] utilized mica within a plasticized polyvinyl chloride matrix. The thermal conductivity of the P-PVC/mica composites exhibited a consistent linear progression and reached a value of 0.59 W/mK as determined by the hot wire method.

Suplicz et al. [42] created a polypropylene with micro-sized ceramic powders of titanium-dioxide. The thermal conductivity of the samples was measured with the hot plate method and the results were calculated with Fourier's law. As a result, the coefficient increased from 0.25 W/mK to 0.64 W/mK. Besides, Hou et al. [43] developed a copper-doped polyethyleneglycol impregnated with titanium dioxide microspheres. The thermal conductivity was investigated using a Hot Disk TPS 2500 S and resulted in 0.58 W/mK.

The experimental thermal conductivity was compared to theoretical models that estimate the thermal conductivity of

composites, using the Equations 4 and 5, which is represented in the Table 5. Comparing the data, it can be observed that the Bruggerman mathematical model is closer to the values found in the experiment. This may have occurred because this model was developed specifically for systems of spherical particulate materials, although it can also provide accurate prediction results for other morphologies. Besides, Bruggeman's model assumes that the particles within the material interact with each other and with the surrounding medium in such a way that the effective properties of the composite can be derived from the properties of the individual constituents. On the other hand, De Loor's model assumes that there is no interaction between the particles and that each particle behaves independently within the matrix material [44].

Table 5. Experimental and theoretical thermal conductivity.

Sample	Experimental (W/m.K)	Bruggerman (W/m.K)	De Loor (W/m.K)
PP/APP	0.224 ± 0.007	0.283	0.625
PP/Mica	0.249 ± 0.004	0.267	0.501
PP/TiO_2	0.251 ± 0.001	0.269	0.514

The Bruggeman's model is also more directly associated with the rule of mixtures than the De Loor model. Thus, the variation in the thermal conductivity of the studied samples is more related to the presence of the flame retardants than to the PP matrix. Despite the increase in thermal conductivity with the addition of the tested flame retardants, it shows potential for the application of these plates as thermal insulators, compared to other materials commonly used in the construction industry, as discussed earlier.

Specific Gravity

Table 6 presents the specific gravity results for each of the materials evaluated. For the PP/APP sample, the specific gravity obtained was 0.939 g/cm³, which represented a 3.3% increase compared to the PP specific gravity. The plate with the addition of Mica showed a specific gravity increase of 28.4% compared to PP, while the increase with the addition of TiO_2 was 24.8%.

Table 6. Specific gravity of PP and the samples with flame retardants.

Sample	Specific Gravity ($g.cm^{-3}$)	Deviation compared with PP (%)
PP	0.909 ± 0.001	-
PP/APP	0.939 ± 0.001	3.3
PP/Mica	1.167 ± 0.005	28.4
PP/TiO_2	1.134 ± 0.001	24.8

Considering that a potential use of these plates could be in the construction industry, it is pertinent to make a comparison with materials widely used by this productive sector. On average, the density of wood found in the Brazilian Atlantic Forest varies between 0.6 and 0.8 g/cm³. The densest wood in this forest is attributed to *Psidium cattleianum*, reaching a value of 1.12 g/cm³ [45]. Another material widely used in the construction industry is gypsum, which, according to Material Property Data [38], has a density of approximately 1.25 g/cm³. Considering that the density of the processed plates remained between 0.939 and 1.167 g/cm³, it can be stated that given these densities, this material has a density that is suitable for the desired application.

Conclusions

In this study, it was possible to analyze the different behaviors of PP with various non-halogenated flame retardants. Morphological analyses revealed the dispersion of fillers within the PP. Furthermore, thermogravimetric analysis demonstrated that the presence of different fillers resulted in an increase of the thermal degradation temperature of PP, with an observed increase in the temperature at which PP initiates its degradation in the curves where TiO_2 were added. Besides, the pyrolysis index of PP/TiO_2 and PP/Mica was roughly one-fourth that of PP/APP and about half that of the pure PP sample. The use of APP showed a higher pyrolysis index compared to TiO_2 and mica, which may suggest lower effectiveness in fire protection.

Considering the thermal and physical characteristics analyzed, both TiO_2 and mica have proven to be viable options as flame retardants for PP, with potential for specific applications in the construction industry. The fire reaction test showed that the fillers were not sufficient to extinguish the flames. However, it was noted that TiO_2 promotes the formation of char on the plates, a good indicator that with further studies, this additive may function as a flame retardant with PP.

The addition of different flame retardants did not significantly modify the thermal conductivity of the plates compared to the thermal conductivity of PP found in the literature. It can also be concluded that, under the tested conditions, these materials have satisfactory characteristics as thermal insulators. Regarding the specific gravity of the plates containing flame retardants, it was observed that in the PP/APP plates, there was only a 3.3% increase in density compared to PP, while for the PP/Mica and PP/TiO_2 plates, the increase was 28.4% and 24.8%, respectively. The specific gravity values found for the plates are like or lower than those of other materials widely used in the construction industry, which suggests that the developed materials have the potential for use as partition boards. These technical attributes encourage their use as insulating materials in the construction industry.

Overall, it is evident that mineral fillers exhibit significant characteristics for the polymer industry and can be a more cost-effective alternative in certain applications, as well as showing potential as flame retardants, particularly for TiO_2 filler.

Acknowledgments

The authors would like to thank Clariant Indústria Química for supplying the fire retardant and CNPq (grant number 304647/2022-5) for financial support.

Authors Contribution

A.P. Tonello: Conceptualization, Methodology, Validation, Formal analysis, Investigation; K.G. Tosin: Validation, Formal analysis, Software, Investigation, Writing—original draft preparation. M. Poletto: Conceptualization, Methodology, Resources, Data curation, Writing—review and editing, Visualization, Supervision, Project administration, Funding. All authors have read and agreed to the published version of the manuscript.

Conflicts of Interest

The authors declare that they have no known competing financial interests or personal relationships that could have appeared to influence the work reported in this paper.

References

[1] A. Rodriguez, M. Herrero, M. Asensio, M. Santiago-Calvo, J. Guerrero, E. Cañibano, M. T. Fernandez, K. Nuñez, Cooperative Effect of Chemical and Physical Processes for Flame Retardant Additives in Recycled ABS. *Polymers*, vol 15, pp. 2431, 2023. DOI: 10.3390/polym15112431.

[2] K. Sykam, S. Donempudi, P. Basak, 1,2,3-Triazole rich polymers for flame retardant application: a review. *Journal of Applied Polymer Science*, vol 139, p. e52771, 2022. DOI: 10.1002/app.52771.

[3] Y. Zhang, Y. Lu, P. Wang, Y. Shi, Biomagnification of Hexabromocyclododecane (HBCD) in a coastal ecosystem near a large producer in China: human exposure implication through food web transfer. *Science of the Total Environment,* vol 624, pp. 1213-1220, 2018. DOI: 10.1016/j.scitotenv.2017.12.153.

[4] T. Sormunen, S. Uusitalo, H. Lindström, K. Immonen, J. Mannila, J. Paaso, S. Järvinen, Towards recycling of challenging waste fractions: Identifying flame retardants in plastics with optical spectroscopic techniques. *Waste Management and Research*, vol 40, pp. 1546–1554, 2022. DOI: 10.1177/0734242X221084053.

[5] R. G. Bringel, A. C. B. Ferreira, B. C. Bonse, E. W. Souza, Action of the compatibilizing agent in synergy with the flame retardant in polypropylene compounds. Proceedings of the 22nd Brazilian congress of Engineering and Materials Science, 2016. Natal, RN, Brazil. Natal, CBECiMat (2016) pp. 8656-8665.

[6] G. Amariei, M. L. Henriksen, P. Klarskov, M. Hinge, In-line quantitative estimation of ammonium polyphosphate flame retardant in polyolefins via industrial hyperspectral imaging system and machine learning. Waste *Management,* vol 170, pp. 1–7, 2023. DOI: 10.1016/j.wasman.2023.07.026.

[7] A. B. Morgan, C. A. Wilkie, Fire Retardancy of Polymeric Materials. 2. ed. [s.l.]: CRC Press, 2010.

[8] J. Feng, L. Liu, y. Zhang, Q. Wang, H. Liang, H. Wang, P. Song, Rethinking the pathway to sustainable fire retardants. *Exploration,* vol. 3, 2023. DOI: 10.1002/exp.20220088.

[9] W. Dukarski, I. Rykowska, P. Krzysanowski, M. Gonsior, Flame Retardant Additives Used for Polyurea-Based Elastomers – A Review. *Fire*, vol. 7, pp. 50, 2024. DOI: 10.3390/fire7020050.

[10] M. Heinz, C. Callsen, W. Stöcklein, V. Altstädt, H. Ruckdäschel, Halogen-free flame-retardant cable compounds: influence of magnesium-di-hydroxide filler and coupling agent on eva/lldpe blend system morphology. *Polymer Engineering & Science*, vol. 62, pp. 461–471, 2021. DOI: 10.1002/pen.25858.

[11] A. Skinner, Plastics Additives. 1 ed. [s.l.]: Springer Science and Business Media, 1998. DOI: 10.1007/978-94-011-5862-6.

[12] B. Szadkowski, M. Piotrowska, P. Rybinski, A. Marzec, Natural bioactive formulations for biodegradable cotton eco-fabrics with antimicrobial and fire-shielding properties. *International Journal of Biological Macromolecules,* vol 237, pp. 124143, 2023. DOI: 10.1016/j.ijbiomac.2023.124143.

[13] J. Alongi, J. Tata, A. Frache, Hydrotalcite and nanometric silica as finishing additives to enhance the thermal stability and flame retardancy of cotton. Cellulose, vol 18, pp. 179-190, 2010. *Springer Science and Business Media LLC*. DOI: 10.1007/s10570-010-9473-z.

[14] P. Elumalai, J. Charles, P. S. Kumar, V. U. Shankar, Fabrication of ternary polyaniline-titanium dioxide-polypyrrole (PANI-TiO2-PPy) nanocomposite as an efficient polymer electrode for supercapacitors. *Journal of Applied Polymer Science,* vol 140, 2023. DOI: 10.1002/app.54478.

[15] C. R. S. Oliveira, M. A. Batistella, S. M. G. U. Souza, A. A. U. Souza, Functionalization of cellulosic fibers with a kaolinite-TiO2 nano-hybrid composite via a solvothermal process for flame retardant applications. *Carbohydrate Polymers,* vol 266, pp. 118108, 2021. DOI: 10.1016/j.carbpol.2021.118108.

[16] L. G. Gerasimova, M. V. Maslova, E. S. Shchukina, Mineral Layer Fillers for the Production of Functional Materials. *Materials*, vol 14, pp. 3369, 2021. DOI: 10.3390/ma14123369.

[17] R. Arjmandi, A. Ismail, A. Hassan, A. A. Bakar, Effects of ammonium polyphosphate content on mechanical, thermal and flammability properties of kenaf/polypropylene and rice husk/polypropylene composites. *Construction And Building Materials*, vol 152, pp. 484–493, 2017. DOI: 10.1016/j.conbuildmat.2017.07.052.

[18] S. Khanal, W. Zhang, S. Ahmed, M. Ali, S. Xu, Effects of intumescent flame retardant system consisting of tris (2-hydroxyethyl) isocyanurate and ammonium polyphosphate on the flame retardant properties of high-density

polyethylene composites. *Composites Part A: Applied Science and Manufacturing*, vol 112, pp. 444–451, 2018. DOI: 10.1016/j.compositesa.2018.06.030.

[19] M. M. Rueda, M. Auscher, R. Fulchiron, T. Périé, G. Martin, P. Sonntag, P. Cassagnau, Rheology and applications of highly filled polymers: a review of current understanding. *Progress In Polymer Science*, vol 66, pp. 22 –53, 2017. DOI: 10.1016/j.progpolymsci.2016.12.007.

[20] Y. Chein, J. Li, X. Lai, H. Li, X. Zeng, N-alkoxyamine-containing macromolecular intumescent flame-retardant-decorated ZrP nanosheet and their synergism in flame-retarding polypropylene. *Polymers For Advanced Technologies*, vol 32, pp. 3804–3816, 2021. DOI: 10.1002/pat.5402.

[21] C. Jo, Y. Jang, D. Mun, C. Yu, C. Choe, S. Ri, Preparation of acrylic emulsion coating with melamine polyphosphate, pentaerythritol and titanium dioxide for flame retardant cotton/polyethylene terephthalate blend fabrics. *Polymer Degradation And Stability*, vol 214, pp. 110366, 2023. DOI: 10.1016/j.polymdegradstab.2023.110366.

[22] P. O. Almeida, C. F. Gerardo, A. G. Leão, S. C. A. França, S. F. Santos, D. C. Bastos, Sustainable Composites Based on Recycled High-density Polyethylene/mica. *Materials Research*, vol. 24, 2021. DOI: 10.1590/1980-5373-mr-2020-0418.

[23] R. Sauerwein, Mineral Filler Flame Retardants. Non-Halogenated Flame Retardant Handbook, pp. 75-141, 2014. DOI: 10.1002/9781118939239.ch3.

[24] T. Protásio, M. V. Scatolino, A. C. C. Araújo, A. F. C. F. Oliveira, I. C. R. Figueiredo, M. R. Assis, P. F. Trugilho, Assessing Proximate Composition, Extractive Concentration, and Lignin Quality to Determine Appropriate Parameters for Selection of Superior Eucalyptus Firewood. *Bioenergy Research*, vol 12, pp. 626 –641, 2019. DOI: 10.1007/s12155-019-10004-x.

[25] C. Moon, Y. Sung, S. Ahn, T. Kim, G. Choi, D. Kim, Effect of blending ratio on combustion performance in blends of biomass and coals of different ranks. *Experimental Thermal And Fluid Science*, vol 47, pp. 232–240, 2013. DOI: 10.1016/j.expthermflusci.2013.01.019.

[26] L. Xiang-Guo, M. Bao-Guo, X. Li, H. Zhen-Wu, W. Xin-Gang, Thermogravimetric analysis of the co-combustion of the blends with high ash coal and waste tyres. *Thermochimica Acta*, vol 441, pp. 79–83, 2006. DOI: 10.1016/j.tca.2005.11.044.

[27] O. S. Odebiyi, M. A. Onitiri, E. T. Akinlabi, Theoretical Investigation into the Thermal Conductivity of Particle Filled Polypropylene Composites. Materials *Today: Proceedings*, vol 5, pp. 74–78, 2018.

[28] H. Li, Z. Hu, S. Zhang, X. Gu, H. Wang, P. Jiang, Q. Zhao, Effects of titanium dioxide on the flammability and char formation of water-based coatings containing intumescent flame retardants. *Progress in Organic Coatings*, vol. 78, pp. 318–324, 2015. DOI: 10.1016/j.porgcoat.2014.08.00

[29] H. S. Kim, H. S. Yang, H. J. Kim, H. J. Park, Thermogravimetric analysis of rice husk flour filled thermoplastic polymer composites. *Journal Of Thermal Analysis And Calorimetry*, vol 76, pp. 395–404, 2004.

[30] R. Yang, Y. Liu, J. Yu, K. Wang, Thermal oxidation products and kinetics of polyethylene composites. *Polymer Degradation And Stability*, vol 91, pp. 1651–1657, 2006. DOI: 10.1016/j.polymdegradstab.2005.12.013.

[31] P. L. Oliveira, R. S. Araújo, V. R. Oliveira, J. S. Morais, M. V. Marques, Nanocomposites of Polyethylene Blends Using Organomica. *Macromolecular Symposia*, vol 367, pp. 143–150, 2016. DOI: 10.1002/masy.201500154.

[32] M. Awang, W. R. W. Mohd, OHD, N. Sarifuddin, Study the effects of an addition of titanium dioxide (TiO2) on the mechanical and thermal properties of polypropylene-rice husk green composites. *Materials Research Express*, vol 6, 2019. DOI: 10.1088/2053-1591/ab1173.

[33] H. E. Ali, A. M. Elbarbary, A. M. Abdel-ghaffar, N. A. Maziad, Preparation and characterization of polyvinyl alcohol/polylactic acid/titanium dioxide nanocomposite films enhanced by γ-irradiation and its antibacterial activity. *Journal Of Applied Polymer Science,* vol 139, 2022. DOI: 10.1002/app.52344.

[34] M. F. Mina, S. Seema, R. Martin, M. J. Rahaman, R. B. Sarker, M. A. Gafur, M. A. H. Bhuiyan, Improved performance of isotactic polypropylene/titanium dioxide composites: effect of processing conditions and filler content. *Polymer Degradation And Stability*, vol 94, pp. 183-188, 2009. DOI: 10.1016/j.polymdegradstab.2008.11.006.

[35] F. M. C. Fonseca, P. Patricio, R. L. Oréfice, Effect of incorporating TiO2 nanoparticles on the structure and properties of polypropylene and poly(hydroxybutyrate) blends subjected to accelerated aging tests. Polímeros*: Ciência e Tecnologia*, vol 24, pp. 395–401, 2014.

[36] J. Riaza, J. Gibbins, H. Chalmers; Ignition and combustion of single particles of coal and biomass. Fuel, vol 202, pp. 650–655, 2017. DOI: 10.1016/j.fuel.2017.04.011.

[37] W. Qian, Q. Xie, Y. Huang, J. Dang, K. Sun, Q. Yang, J. Wang; Combustion characteristics of semicokes derived from pyrolysis of low rank bituminous coal. *International Journal Of Mining Science And Technology*, vol 22, pp. 645–650, 2012. DOI: 10.1016/j.ijmst.2012.08.009.

[38] Material Property Data. Plaster; Molded, Dry. Available: <http://www.matweb.com/search/DataSheet.aspx?MatGUID=0e684bc25a1642d0a90aabe41f59b917>. (accessed on: 26 oct. 2023).

[39] T. L. Bergman, A. Lavine, F. Incropera, D. P. Dewitt, Fundamentals of heat and mass transfer. 7. ed. Rio de Janeiro: Ltc, 2014.

[40] Y. Leng, M. Xu, Y. Sun, R. Han, B. Li, Simultaneous enhancement of thermal conductivity and flame retardancy for epoxy resin thermosets through self-assemble of ammonium polyphosphate surface with graphitic carbon nitride. *Polymers For Advanced Technologies*, vol 30, pp. 2468–2479, 2019. DOI: 10.1002/pat.4694.

[41] H. Zhang, J. Zhang, Rheological behaviors of plasticized polyvinyl chloride thermally conductive composites with oriented flaky fillers: a case study on graphite and mica. *Journal of Applied Polymer Science*, vol 139, 2022. DOI: 10.1002/app.52186.

[42] A. Suplicz, F. Szabo, J. G. Kovacs, Injection molding of ceramic filled polypropylene: the effect of thermal conductivity and cooling rate on crystallinity. *Thermochimica Acta*, vol 574, pp. 145–150, 2013. DOI: 10.1016/j.tca.2013.10.005.

[43] J. Hou, Y. Wang, J. Liu, J. Zhao, S. Long, J. Hao, Enhanced thermal conductivity of copper-doped polyethylene glycol/urchin-like porous titanium dioxide phase change materials for thermal energy storage. International *Journal of Energy Research*, vol 44, pp. 1909–1919, 2019. DOI: 10.1002/er.5045.

[44] N. Kucukdogan, L. Aydin, M. Sutcu, Theoretical and empirical thermal conductivity models of red mud filled polymer composites. *Thermochimica Acta,* vol. 665, pp. 76 –84, 2018. DOI: 10.1016/j.tca.2018.05.013.

[45] D. L. Padilha, P. M. Júnior, A gap in the woods: wood density knowledge as impediment to develop sustainable use in atlantic forest. *Forest Ecology And Management*, vol 424, pp. 448–457, 2018. DOI: 10.1016/j.foreco.2018.05.012.